http://dx.doi.org/10.5012/bkcs.2012.33.5.1741

Syntheses and Characterizations of Serine and Threonine Capped Water-Dispersible ZnS:Mn Nanocrystals and Comparison Study of Toxicity Effects on the growth of *E. coli* by the Methionine, Serine, Threonine, and Valine Capped ZnS:Mn Nanocrystals

Eunju Lim,[†] Sanghyun Park, Jonghoe Byun,[‡] and Cheong-Soo Hwang[*]

Department of Chemistry, [†]Department of Applied Physics, and [‡]Department of Molecular Biology, Dankook University, Center for Photofunctional Energy Materials (GRRC program), Institute of Nanosensor and Biotechnology, Gyunggi-do 448-701, Korea. [*]E-mail: cshwang@dankook.ac.kr
Received November 15, 2011, Accepted March 9, 2012

Water-dispersible ZnS:Mn nanocrystals were synthesized by capping the surface of the nanocrystals with conventional aminoacids ligands: serine and threonine. The aminoacids capped ZnS:Mn nanocrystal powders were characterized by XRD, HR-TEM, EDXS, ICP-AES and FT-IR spectroscopy. The optical properties were also measured by UV/Vis and solution photoluminescence (PL) spectroscopies in aqueous solvents. The solution PL spectra showed broad emission peaks around 600 nm with PL efficiencies of 9.7% (ZnS:Mn-Ser) and 15.4% (ZnS:Mn-Thr) respectively. The measured particle sizes for the aminoacid capped ZnS:Mn nanocrystals by HR-TEM images were about 3.0-4.0 nm, which were also supported by Debye-Scherrer calculations. In addition, cytotoxic effects of four aminoacids capped ZnS:Mn nanocrsystals over the growth of wild type *E. coli* were investigated. Although toxicity in the form of growth inhibition was observed with all the aminoacids capped ZnS:Mn nanocrystals at higher dose (1 mg/mL), ZnS:Mn-Met and ZnS:Mn-Thr appeared non-toxic at doses less than 100 μg/mL. Low biological toxicities were seen at doses less than 10 μg/mL for all nanocrystals.

Key Words : ZnS:Mn nanocrystal, Amino acid capping, Water-dispersible nanocrystal, Orange emitting nanophosphor, Toxicity of nanocrystal

Introduction

An orange light emitting manganese ion doped zinc sulfide nanocrystallite, ZnS:Mn, is of special interest due to its high quantum efficiency and colloidal stability at ambient temperature,[1] which are critical properties required to be applied for general photo-voltaic[2] and electro-luminescence devices.[3] Considerable progress has been made in the synthetic methods for the ZnS:Mn naonocrystal materials including gas, solid state, and aqueous solution reactions via organometallic thermal decomposition routes. However, these methods often require high temperatures, pressures and even use of extremely toxic chemical substances.[4]

Water-dispersible semiconductor nanocrystals were developed for fluorescent labeling technologies especially to be applied in biological area.[5,6] Unfortunately, most highly luminescent semiconductor nanocrystals are grown in hydrophobic media so that they are hardly compatible with biological systems. There are several reports of solubilized hydrophobic nanocrystals in water.[7,8] The most common synthetic scheme for the water-dispersible nanocrystal is to use polar surface capping ligands such as mercaptoacetate (MAA) and sulfodiisooctyl succinate (AOT) molecules to form a micelle structure where the negative charges are distributed on the surface. In addition, it was shown that the photoluminescence efficiency for the AOT capped ZnS:Mn nanocrystal increased up several times after the surface modification.[9] This phenomenon resulted from the additional energy transfer of surfactant to Mn^{2+} metal ion as well as reducing the energy loss due to non-radioactive transition by the surface modification.

Amino acid ligands such as histidine[10] and cysteine[11] have been developed as surface capping agents for undoped ZnS nanocrystals. They were found to be very effective capping ligands in the synthesis of narrow range size distributed nanocrystals, which is difficult to achieve in aqueous solution due to different dissociation constants for ZnS and MnS in water. A brief description of the synthesis of histidine coordinated ZnS:Mn nanocrystal has been appeared once in a literature.[12] Previously, we have reported syntheses and optical characterizations of arginine, cysteine, histidine and methionine capped ZnS:Mn nanocrystals.[13] In that paper, we showed that we were able to directly synthesize water-dispersible ZnS:Mn nanocrystals by using commercially available aminoacids as surface capping ligands in aqueous solution, regardless of the different nature of the aminoacids molecules in terms of acidity, bulkiness, and presence of aromatic rings. In addition, more recently, we also have reported toxicological study for ZnS:Mn-Cys and ZnS:Mn-His nanocrystals on the growth of *E. coli* bacteria and mammalian cells.[14] In that paper we tried to show that the both aminoacids capped ZnS:Mn nanocrystals are not toxic enough to be used for

biological labeling study and even for environment-friendly commercial LED devices. In this paper, we like to report syntheses of new ZnS:Mn nanocrystals capped with threonine and serine. Moreover, toxicity effects on the growth of *E. coli* by four amino acids capped ZnS:Mn nanocrystals, which are methionine, serine, threonine, and valine, were also investigated. In this paper, we tried to enlarge the previous biological toxicity study for the aminoacids capped ZnS:Mn nanocrystals so that we can show that aminoacid capping for ZnS:Mn nanocrystal genarally induces lower biological toxicity than other polar ligands such as MAA and AOT, which have been more frequently used to synthesize water-soluble inorganic semiconductor nanocrystals.

Experimental

All the solvents except deionized water were purchased from Aldrich (reagent grade) and distilled prior to use. The starting materials including L-threonine, L-serine, $ZnSO_4$, $MnSO_4$, and Na_2S were purchased from Aldrich and used as received. The wild type of *E. coli* K-12 was purchased from the Korean Culture Center of Microorganisms (KCCM 40939).

The UV/Vis absorption spectrum was recorded on a Perkin Elmer Lamda 25 spectrophotometer equipped with a deuterium/tungsten lamp. The FT-IR spectrum was recorded on a Perkin Elmer spectrophotometer equipped an attenuated total reflection (ATR) unit. The solution photoluminescence spectra were taken by a Perkin Elmer LS-45 spectrophotometer equipped with a 500 W Xenon lamp, 0.275 m triple grating monochrometer, and PHV 400 photomultiplier tube. HR-TEM images were taken with a JEOL JEM 1210 electron microscope with a MAG mode of 1000 to 800000, and the accelerating voltage was 40-120 kV. The samples for the TEM were prepared via dispersion into methanol solvent and placement on a carbon-coated copper grid (300 Mesh) followed by drying under vacuum. In addition, the elemental compositions of the nanocrystals were determined by EDXS (Energy Dispersive X-ray Spectroscopy) spectra which were obtained via an EDXS collecting unit equipped in the HR-TEM, with a Si (Li) detector in IXRF 500 system. ICP-AES elemental analyses for the ZnS:Mn-MAA and ZnS:Mn-MPA nanocrystals were performed by Optima-430 (Perkin Elmer) spectrometer equipped with Echelle optics system and Segmented array charge coupled device (SCD) detector. To prepare a sample of corresponding nanocrystal, a 0.5 mL of the concentrated nanocrystal solution was mixed with 9.5 mL of concentrated nitric acid over the period of 3 days. After which 0.5 mL of the digested solution is placed in a 9.5 mL of nanopure-water.

Syntheses of Amino Acids Capped ZnS:Mn Nanocrystals. Preparation procedures are slightly modified from the methods to prepare L-valine capped ZnS:Mn nanocrystal via formation of zinc (II)-amino acid coordinated complexes as reactive intermediates in aqueous solution.[15] A solution of $ZnSO_4 \cdot 5H_2O$ (1.44 g, 5 mmol) in 50 mL of water was slowly added to a 50 mL aqueous mixture solution containing 10 mmols of amino acids and NaOH (0.40 g, 10 mmol) at 5 °C (ice-water bath). The solution was warmed up to ambient temperature after 1 hour stirring. Each resulting white powder was redissolved in a 50 mL of warm (*ca.* 60 °C) 1 M Tris buffer (Aldrich) solution. In another flask, $MnSO_4 \cdot H_2O$ (0.02 g, 0.1 mmol) and Na_2S (0.40 g, 5 mmol) was dissolved in a 20 mL of 0.01 M HCl solution. Then the mixture was transferred to the flask containing Zn-amino acid complexes under vigorous stirring. The resulting solution refluxed for 20 hours. Slow cooling to ambient temperature and an addition of ethanol solution resulted in yellow-white precipitations at the bottom of the flask. Finally, the obtained solids were separated via centrifuge and decanting the supernatant. Then the solids were dried for 24 hours in a vacuum oven. The obtained experimental data are summarized in Table 1.

Photoluminescence Efficiency Measurements and Calculations. The PL efficiencies for the amino acid capped ZnS:Mn nanocrstals were measured and calculated by following the same method reported by Williams *et al.*[16] which is to calculate a relative quantum yield by comparing to a standard material in literature,[17] 0.1 M solution of quinine sulfate in H_2SO_4 (Fluka) in our case, whose emission wave length and reported absolute quantum yield are 550-600 nm and 0.546 (at 22 °C) respectively. The used excitation wavelength for the standard (quinine sulfate) solution was obtained from the UV/Vis spectrum for each aminoacid capped ZnS:Mn nanocrystal. The emission spectra for both standard and aminoacid capped ZnS:Mn nanocrystal were recorded at five different concentrations in aqueous solvents. Then we plotted a graph of integrated fluorescence intensity versus absorbance for both samples obtained at different concentrations. As a result we were able to obtained straight lines with fairly constant gradients. Finally, the relative PL efficiencies were calculated by using the following equation:

$$\Phi_x = \Phi_{ST}\left(\frac{Grad_x}{Grad_{ST}}\right)\left(\frac{\eta_x^2}{\eta_{ST}^2}\right)$$

In this equation, Φs represent PL efficiencies. The

Table 1. Experimental data summary for the amino acids capped ZnS:Mn nanocrystals

	ZnS:Mn (Ser)	ZnS:Mn (Thr)	ZnS:Mn (Met) Ref. 13	ZnS:Mn (Val) Ref. 15
UV/Vis (λ_{max}, nm)	309	315	317	305
PL emission wavelength (nm)	595	600	576	558
PL efficiency (%)	9.7	15.4	7.1	15.8
HR-TEM image (average particle size, nm)	2.9	3.2	8.3	3.3

subscript ST and *x* denote the standard (quinine sulfate) and the corresponding aminoacid capped ZnS:Mn nanocrystal respectively. In addition, 'Grad' indicates the gradient from the plot integrated fluorescence intensity versus absorbance, and 'η' represents the refractive index of the solvent, which we could eliminate this factor by using the same solvent for both standard and the nanocrystal.

Batch Culture of *Escherichia coli*. *E. coli* K-12 strain was grown in 5 mL of nutrient broth (beef extract 3 g/L, peptone 5 g/L, NaCl 10 g/L) with shaking at 37 ºC for 16 hrs. Each amino acid was dissolved in 5 mL of the nutrient broth to give a concentration of 20 mg/mL at 37 ºC and this stock solution was used to achieve different concentrations in the bacterial culture (0 to 1 mg/mL, final 18 mL). After complete dissolution of nanocrystals, sufficiently grown *E. coli* K-12 (16 hr) was inoculated into each nutrient broth. To plot growth curve, the turbidity of the culture was checked every 30 min by measuring optical density at 600 nm using SpectraMax M2e microplate reader (Molecular Devices). The study was performed in triplicate.

Statistical Analysis. The data were expressed as means ± SEM. Results were analyzed with GraphPad Prism statistics software (GraphPad Software, Inc., San Diego, CA, USA). Student's *t*-test was used to evaluate statistical differences between the groups. A *P* value less than 0.05 was considered statistically significant.

Results and Discussions

Figure 1(a) presents UV-visible absorption spectra of ZnS:Mn-Ser and ZnS:Mn-Thr nanocrystals. The maximum absorption for the ZnS:Mn-Ser and ZnS:Mn-Thr were 309 nm and 315 nm respectively. In addition, Figure 1(b) presents the room temperature solution PL spectra obtained from the corresponding amino acids capped ZnS:Mn in aqueous solution, in which broad emission peaks appeared at 595 nm (ZnS:Mn-Ser) and 600 nm (ZnS:Mn-Thr) wavelengths, respectively. The excitation spectra were also obtained when the scanning wavelengths of the light source were fixed at 595 nm (ZnS:Mn-Ser) and 600 nm (ZnS:Mn-Thr). The second-order diffraction peaks of the excitation wavelengths appeared around 600-650 nm in both PL spectra; however, they did not interrupt to identify the emission peaks by the nanocrystals. The observed large Stoke shifts for the serine and threonine capped ZnS:Mn nanocrystals are attributed to the $^4T_1 \rightarrow {}^6A_1$ transition of the Mn^{2+} doping agent.[18] In addition, the corresponding PL efficiencies were also measured and calculated by comparing to that for the 0.1 M quinine sulfate standard in sulfuric acid solution as described in the experimental section.[17] As a result, the obtained PL efficiencies were 9.7% (ZnS:Mn-Ser) and 15.4% (ZnS:Mn-Thr) respectively, which are close to that for ZnS:Mn-Met (7.1%)[13] and ZnS:Mn-Val (15.8%).[15]

The particle sizes of the corresponding amino acids capped ZnS:Mn nanocrystals were measured via HR-TEM images presented in Figure 2. Unfortunately, the obtained HR-TEM images are not so clearly showing individual discrete particles due to existence of some aggregates of the aminoacids capped ZnS:Mn nanocrystal particles, which were possibly caused by hydrogen bonding interactions between aminoacid capping molecules. However, we were able to find some of fringe images of the particles by maximum enlarging the HR-TEM images, and we also tried to measure particle sizes as many as we could to obtain the average particle sizes from the images. The measured average particle sizes are 2.9 nm (ZnS:Mn-Ser) and 3.2 nm (ZnS:Mn-Thr), which are similar to that for the valine capped ZnS:Mn nanocrystal (3.3 nm in average). In addition, we also performed Debye-Scherrer calculations for both aminoacids capped ZnS:Mn nanocrystals by using obtained XRD peaks to support our measurements of the particle sizes.[19] From measured full width at half maxima (FWHM) of selected XRD peaks, we obtained calculated average particle sizes for ZnS:Mn-Ser and ZnS:Mn-Thr nanocrystals, which were 3.6 nm and 3.9 nm respectively. It is notable to mention that the present aggregates could cause extra broadening of PL emission peaks and XRD peaks as shown in corresponding diagrams in this paper.

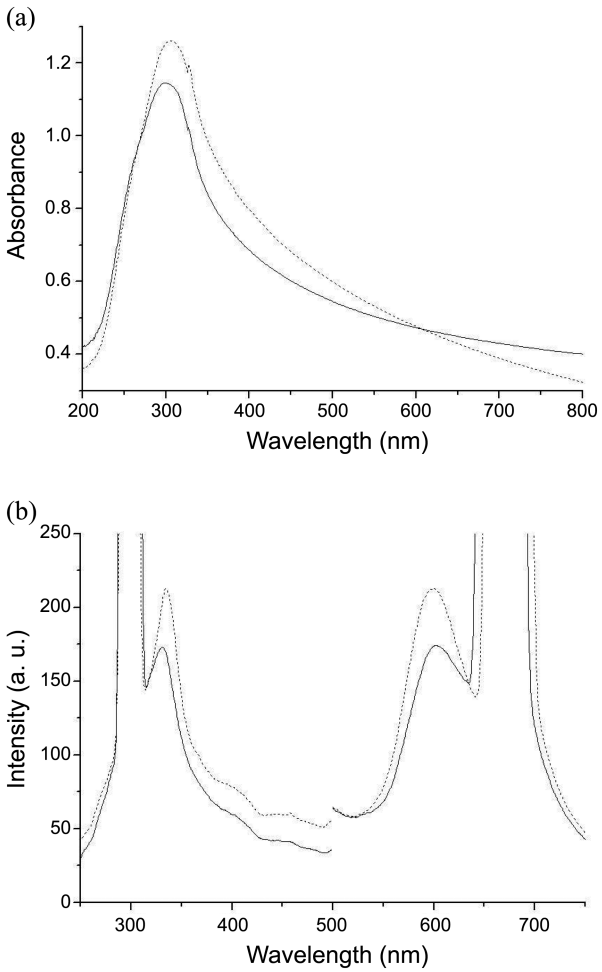

Figure 1. (a) UV-Vis absorption spectra of ZnS:Mn-Ser (solid line) and ZnS:Mn-Thr (dots). (b) Room temperature photoluminescence excitation and emission spectra of ZnS:Mn-Ser (solid lines) and ZnS:Mn-Thr (dots).

(a) ZnS:Mn-Ser

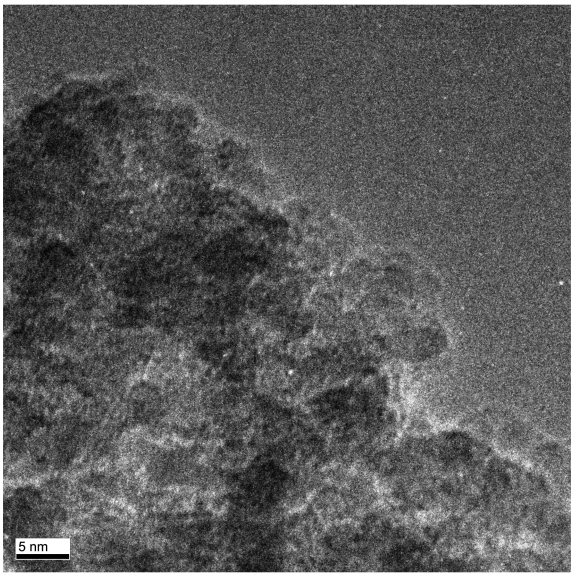

(b) ZnS:Mn-Thr

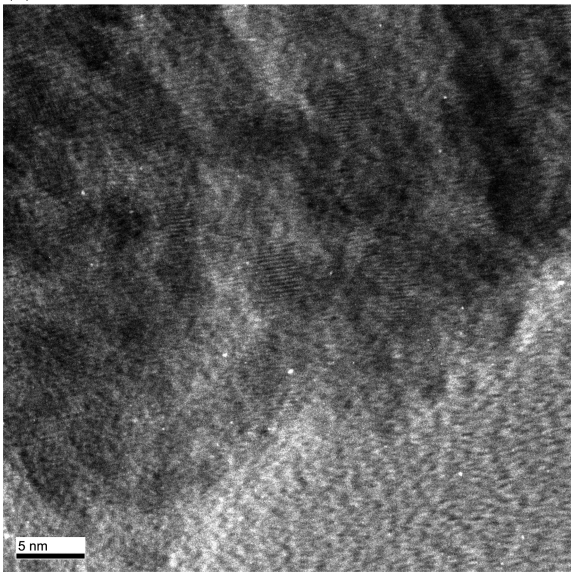

Figure 2. HR-TEM images of the amino acids capped ZnS:Mn nanocrystals. The scale bar represents 5 nm; (a) ZnS:Mn-Ser and (b) ZnS:Mn-Thr.

The EDXS (energy-dispersive X-ray spectroscopy) diagrams were provided in Figure 3, which showed that the elemental compositions of the corresponding product solids. The diagrams confirm the formation of the ZnS:Mn nanocrystals in solid state. In addition, the EDXS elemental analysis also showed that the doping percentages of the manganese ions in the measured ZnS:Mn nanoparticles are 1.65% (ZnS:Mn-Ser) and 2.30% (ZnS:Mn-Thr) respectively. In addition, ICP-AES analyses for both aminoacids capped ZnS:Mn nanocrystals were performed for more precise elemental analyses. The obtained Zn and Mn concentrations were converted into the molar ratio, which revealed the average doping percentage of Mn ion was 3.2% and 2.7% for ZnS:Mn-Ser and ZnS:Mn-Thr repectively, which showed little bit

(a)

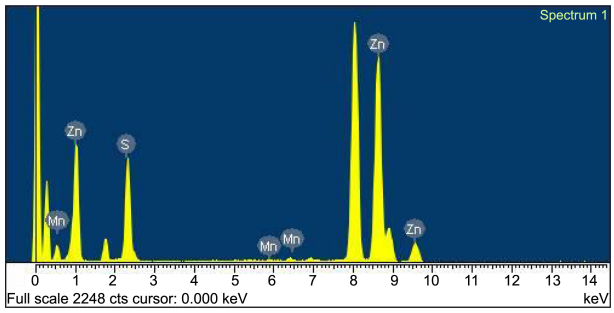

(b)

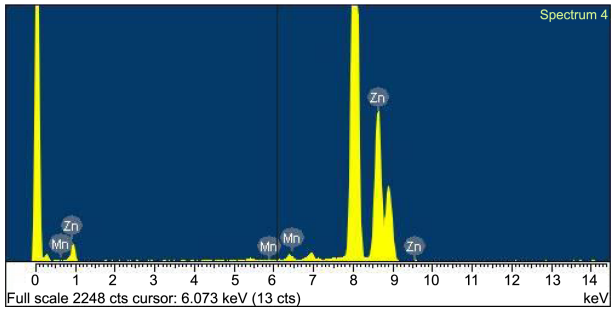

Figure 3. EDXS spectra for the amino acids capped ZnS:Mn nanocrystals: (a) ZnS:Mn-Ser and (b) ZnS:Mn-Thr.

different values from the EDXS analyses. The obtained concentrations of Mn ions, by the ICP-AES analyses, were probably fully resulted from the doped Mn ions in the aminoacids capped ZnS nanocrystal lattices since we did not observe any other peaks caused by Mn precursor ($MnSO_4$) or by possible side products (*e.g.* MnS or other aminoacid-Mn complexes) in the present XRD diagrams for the amino-acids capped ZnS:Mn nanocrystals. It has been reported that the amount of the dopant usually affects the emission wave length for the bulk ZnS:Mn solid.[20] However, in our case, the effect of the amount of the dopant was not so significant since the emission wavelengths for the amino acids capped ZnS:Mn nanocrystals were very similar to each other.

Figure 4 shows the wide angle X-ray diffraction (XRD) patterns of powder samples of the amino acids capped ZnS:Mn nanocrystals. In those diagrams, mostly appeared peaks are broad; however, it is a well known feature for most low-dimensional nano-sized solid materials. Even so, there were obviously indexable peaks such as (111), (220) and (311) planes in those diagrams indicating that the nanocrystals are in cubic zinc blende phases for serine and threonine capped ZnS:Mn nanocrystals.[21]

The corresponding aminoacid ligands on the surface of the ZnS:Mn nanocrystals were characterized by FT-IR spectroscopy as shown in Figure 5. The present IR peaks were listed and accordingly assigned in Table 2 and 3. The individual peaks were assigned by comparing that of corresponding free aminoaicd molecule associated with theoretical calculations.[22,23] For ZnS:Mn-Ser and ZnS:Mn-Thr nanocrystals, the strong peaks appeared around 3200, and 2300 cm^{-1} were assigned as stretching vibrational peaks of zinc coordinated -NH_2 groups. In addition, the metal coordinated -COO^- groups

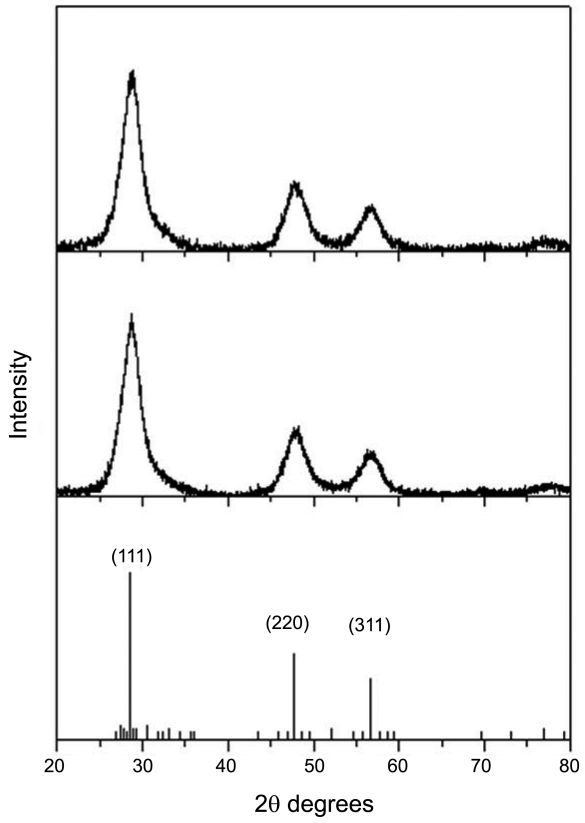

Figure 4. Powder X-ray diffraction pattern diagrams for the amino acids capped ZnS:Mn nanocrystals; ZnS:Mn-Ser (top); Middle; ZnS:Mn-Thr (middle); and bulk ZnS solid in a cubic zinc blende phase (bottom).

in the surface capping aminacid molecules appeared around 1400 and 1300 cm^{-1} for both nanocrystals. The peaks of the NH_2 and COO groups in ZnS:Mn-aminoacid nanocrystals were slightly down shifted from that of corresponding free aminoacid molecules since they are coordinated to heavier zinc metal ions on the surface of the nanocrystals.[24] Similar phenomena have been observed in other aminoacids capped ZnS:Mn nanocrystals.[13,15] To remove any uncoordinated or unreacted aminoacid molecules, the centrifuged white solids were washed several times with cold alcohol/water mixture solutions rapidly. As a result, we were not able to find peaks resulted from the precursors, free aminoacid molecules, in the FT-IR spectra as demonstrated in the Figure 5. In addition, the spectra confirmed that all of the aminoacid molecules are attached on the surface of the ZnS:Mn nanocrystals to provide a water dispersible nature for the originally hydrophobic ZnS:Mn nanocrystals.

Next, these amino acid-capped nanocrystals were evaluated for their potential toxicities in *E. coli* which are typical bacteria associated with human. For these experiments, optical density (OD) 600 method was employed, which measures degree of turbidity of the nutrient broth by filling with growing bacteria.[25] The more turbid solution scatters the more scanned light so that the intensities of the passing light decrease as bacterial growth. Usually the spectroscopic bacterial growth monitoring is performed at 550-600 nm

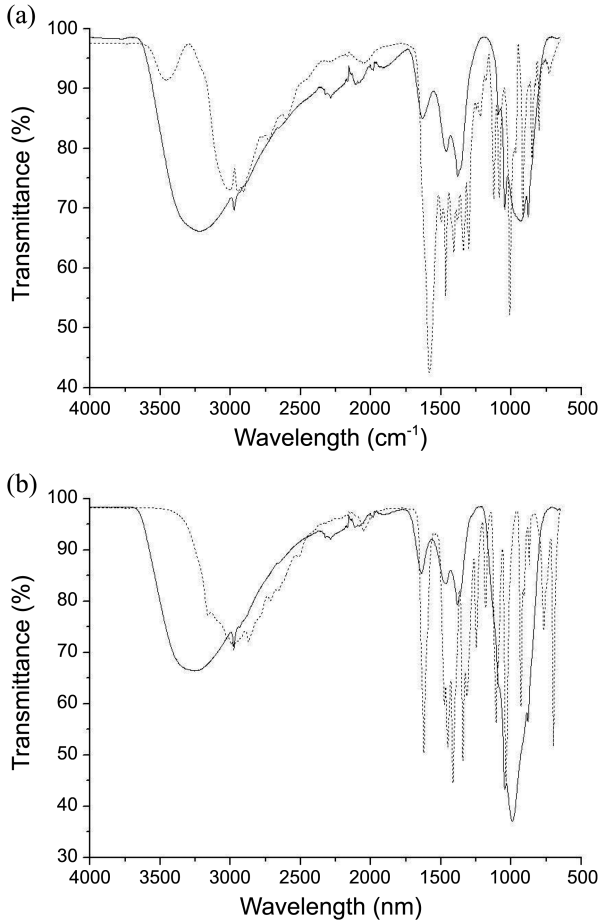

Figure 5. FT-IR spectra of the amino acids capped ZnS:Mn nanocrystals with corresponding free aminoacids; (a) ZnS:Mn-Ser (solid) and free Ser (dots); (b) ZnS:Mn-Thr (solid) and free Thr (dots).

Table 2. FT-IR peak lists and analyses for ZnS:Mn-Ser and free serine

ZnS:Mn-Ser (cm^{-1})	Free serine (cm^{-1})	Assignments[22]
N/A	3429(m)	νO-H
3220(br)	3350(s)	νN-H
2974(m)	2956(s)	νC-H
N/A	2595(m)	νO-H
2286(w)	2346(m)	νN-H
2107(w)	2188(m)	νN-H
2086(w)	2148(m)	νN-H
1633(s)	1642(s)	γN-H
1462(s)	1580	νCOO^-
1383(s)	1434(s)	νCOO^-
1091(w)	1090	νC-O
1047(m)	1048(m)	δN-H
935(s)	973(s)	νC-N
879(s)	856(s)	νC-C

br = broad, w = weak, m = medium, s = strong, ν = stretching, ω = wagging, δ = bending, γ = rocking. N/A (not appeared)

working range because the nutrient broth has a very low OD value at this wave length region.[26] Since the ZnS:Mn nano-

Table 3. FT-IR peak lists and analyses for ZnS:Mn-Thr and free threonine

ZnS:Mn-Thr (cm^{-1})	Free threonine (cm^{-1})	Assignments[23]
3256(br)	3169(m)	νN-H
2976(m)	2998(m)	νN-H
N/A	2947(w)	νC-H
2565(w)	2882(w)	νC-H
2324(w)	2790(w)	νN-H
2286(w)	2753(w)	νN-H
1638(s)	1651(s)	δN-H
1460(m)	1480(s)	νCOO-
1383(s)	1388(s)	νCOO-
1046(m)	1093(s)	νCCN
991(s)	932(s)	νCC
880(m)	871(s)	νCC

br = broad, w = weak, m = medium, s = strong, ν = stretching, ω = wagging, δ = bending, γ = rocking. N/A (not appeared)

crystals do not emit any light by scanning the 600 nm light source, they don't interrupt the OD measurements at all; therefore, this method should be valid for estimating the biological toxicity of the aminoacids capped ZnS:Mn nanocrystals.

As shown in Figure 6, little toxicities were seen at concentrations less than 10 g/mL in all groups. However, growth inhibition was apparent at highest concentration (1 mg/mL), which was greater in ZnS:Mn-Ser and ZnS:Mn-Val groups than in ZnS:Mn-Thr or ZnS:Mn-Met. In 10-fold less concentration (100 g/mL), the toxicity was highest in ZnS:Mn-Ser group, followed by ZnS:Mn-Val, ZnS:Mn-Thr, and ZnS:Mn-Met groups.

Conclusion

We have successfully synthesized water-dispersible ZnS:Mn nanocrystals by capping the originally hydrophobic surface of the nanocrystals with four kinds of amino acids molecules: serine, threonine, methionine and valine. These colloidal nanocrystals were measured for their optical properties by UV/Vis, room temperature solution PL spectroscopies, and further obtained powders were characterized by XRD, HR-TEM, EDXS, and FT-IR spectroscopy analyses. One of the reasons that we synthesized the water-soluble ZnS:Mn semiconductor nanocrystals is to bind them to biomolecules, such as DNA and protein, so that they can be used as a biosensor material. For these biological applications, we studied their potential toxic effects in typical enteric bacteria. Although toxicity in the form of growth inhibition was observed with all groups at higher dose (1 mg/mL), the ZnS:Mn nanocrystals capped with methionine

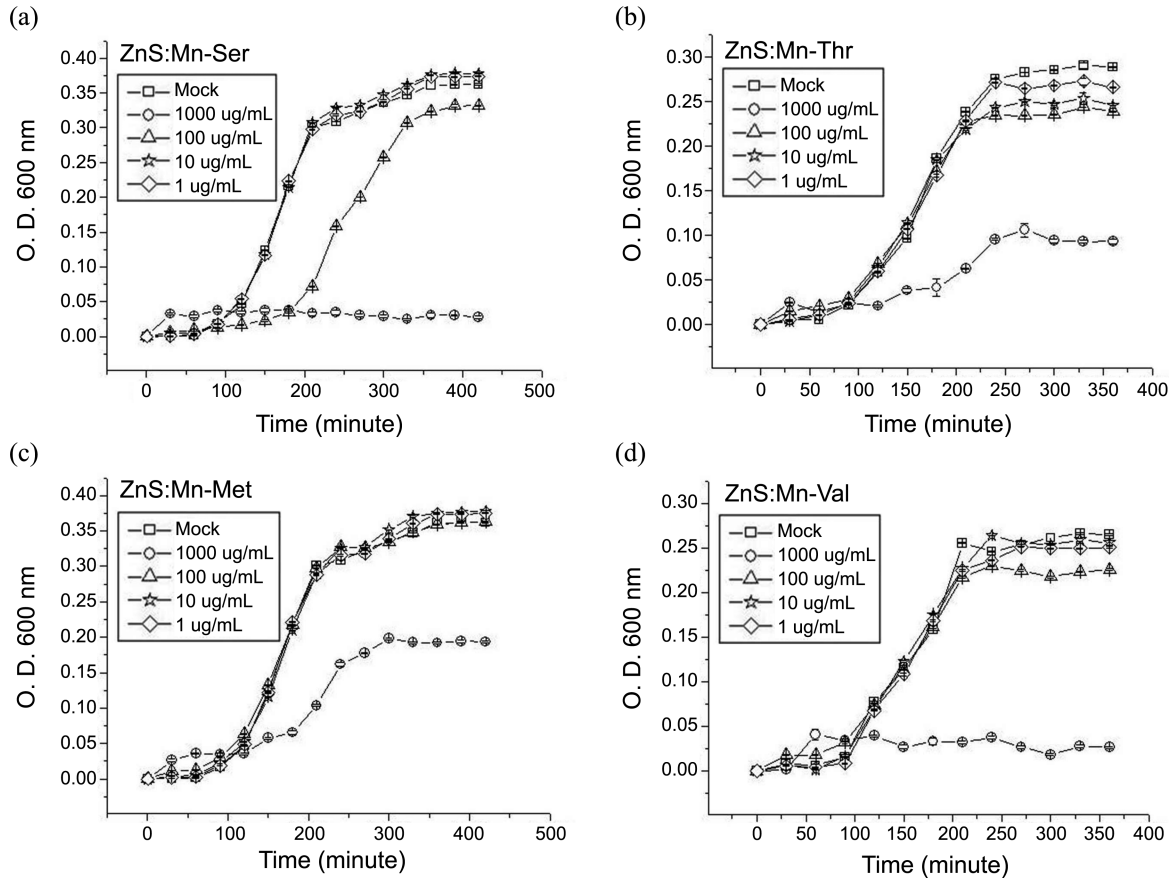

Figure 6. Concentration dependent toxicity of nanocrystals in *E. coli*.; (a) ZnS:Mn-Ser, (b) ZnS:Mn-Thr (c) ZnS:Mn-Met, and (d) ZnS:Mn-Val. The notation of "Mock" means 0 μg/mL of nanocrystal soluitons.

and threonine appeared safe at doses less than 100 mg/mL. Little toxicities were seen at doses less than 10 mg/mL in all groups. Further studies are required to unveil the mechanism behind the increased safety associated with particular amino acids.

Acknowledgments. This research was supported by the GRRC program of Gyonggi Province [GRRC-Dankook-2011-B02].

References

1. Hwang, J. M.; Oh, M. O.; Kim, I.; Lee, J. K.; Ha, C.-S. *Curr. Appl. Phys*. **2005**, *5*, 31.
2. Breen, M. L.; Dinsmore, A. D.; Pink, R. H.; Qadri, S. B.; Ratna, B. R. *Langmuir* **2001**, *17*, 903.
3. Hoffman, A. J.; Mills, G.; Yee, H.; Hoffmann, M. R. *J. Chem. Phys*. **1992**, *96*, 5546.
4. Yu, S. H.; Wu, Y. S.; Yang, J. C*hem. Mater.* **1998**, *9*, 2312.
5. Gerion, D.; Pinaud, F.; Williams, S. C.; Parak, W. J.; Zanchet, D.; Weiss, S.; Alivisatos, A. P. *J. Phys. Chem. B* **2001**, *195*, 8861.
6. Jun, Y. W.; Jang, J. T.; Cheon, J. W. *Bull. Korean Chem. Soc*. **2006**, *27*, 961.
7. Mitchell, G. P.; Mirkin, C. A.; Letsinger, R. L. *J. Am. Chem. Soc*. **1999**, *121*, 8122.
8. Kho, R.; Nguyen, L.; Torres-Martinez, C. L.; Mehra, R. K. *Biochem. Biophys. Res. Commun*. **2000**, *272*, 29.
9. Chen, C. C.; Yet, C. P.; Wang, H. N.; Chao, C. Y. *Langmuir* **1999**, *15*, 6845.
10. Bae, W.; Mehra, R. K. *J. Inorg. Biochem*. **1998**, *70*, 125.
11. Bhargava, R. N.; Gallagher, D. *Phys. Rev. Lett*. **1994**, *72*, 416.
12. Yi, G.; Sun, B.; Yang, F.; Chen, D. *J. Mater. Chem*. **2001**, *11*, 2928.
13. Lee, J. H.; Kim, Y. A.; Kim, K.; Huh, Y. D.; Hyun, J. W.; Kim, H. S.; Noh, S. J.; Hwang, C. S. *Bull. Korean Chem. Soc.* **2007**, *28*, 1091.
14. Kong, H. Y.; Kim, S. Y.; Byun, J.; Hwang, C. S. *Bull. Korean Chem. Soc.* **2010**, *32*, 53.
15. Hwang, C. S.; Lee, N. R.; Kim, Y. A.; Park, Y. B. *Bull. Korean Chem. Soc*. **2006**, *27*, 1809.
16. Williams, A. T. R.; Winfield, S. A.; Miller, J. N. *Analyst*. **1983**, *108*, 1067.
17. Melhuish, W. H. *J. Phys. Chem*. **1961**, *65*, 229.
18. Chen, W.; Su, F.; Li, G.; Joly, A. G.; Malm, J.-O.; Bovin, J.-O. *J. Appl. Phys.* **2002**, *92*, 1950.
19. (a) *International Union of Crystallography in International Tables for X-Ray Crystallography*, Part III; Netherlands, Dordrecht, 1985; p 318 (b) Qinghong, Z.; Lian, G.; Jinkun, G. *Appl. Catal. B Environ.* **2000**, *26*, 207.
20. Kushida, T.; Tanak, Y.; Oka, Y. *Sol. Stat. Commun*. **1974**, *14*, 617.
21. Zhuang, J.; Zhang, X.; Wang, G.; Li, D.; Yang, W.; Li, T. *J. Mater. Chem*. **2003**, *13*, 1853.
22. Jarmelo, S.; Reva, I.; Carey, P. R.; Fausto, R. *Vib. Spectro.* **2007**, *43*, 395.
23. Silva, B. L.; Freire, P. T. C.; Melo, F. E. A.; Guedes, I.; Silva, M. A. A.; Filho, J. M.; Moreno, A. D. J. *Braz. J. Phys*. **1998**, *28*, 19.
24. (a) Moszczenski, C. W.; Hooper, R. J. *Inorg. Chim. Acta* **1983**, *70*, 71. (b) Nakamoto, K. *Infrared and Raman Spectra of Inorganic and Coordination Compounds*, Part B, 5th ed.; Wiley: 1997; p 59.
25. Begot, C.; Desnier, I.; Daudin, D. J.; Labadie, J. C.; Lebert, A. *J. Microbiol. Meth.* **1996**, *25*, 225.
26. Zabic, M.; Kukric, Z.; Topalic-Trivunovic, L. *Chem. Ind. & Chem. Eng. Quart.* **2009**, *15*, 251.